Available online at website: https://journal.bcrec.id/index.php/bcrec

Bulletin of Chemical Reaction Engineering & Catalysis, 21 (2) 2026, 412-427

Original Research Article

Enhancing Enzymatic Digestibility and Lignin Production of Oil Palm Empty Fruit Bunch (OPEFB) by Green Deep Eutectic Solvent

Candra Wijaya[1,2], Urania Noor Lintang Pertiwi[1], Tabina Raissa Apol[1], Ika Putri Nikmatur Rohmah[1], Maktum Muharja[1], Tri Widjaja[1], Lieke Riadi[2], Arief Widjaja[1*]

[1]*Department of Chemical Engineering, Faculty of Industrial Technology, Institut Teknologi Sepuluh Nopember, Surabaya 60111, Indonesia.*
[2]*Departement of Chemical Engineering, Faculty of Engineering, Universitas Surabaya (UBAYA), Jalan Raya Kalirungkut (Tenggilis), Surabaya 60293, Indonesia.*

Received: 8th December 2025; Revised: 21th February 2026; Accepted: 22th February 2026
Available online: 25th February 2026; Published regularly: August 2026

Abstract

Oil palm empty fruit bunch (OPEFB) is an abundant lignocellulosic residue whose high lignin content restricts its bioconversion into sugars and value-added products. Deep eutectic solvents (DESs), particularly choline chloride–lactic acid, offer a green and tunable platform for selective delignification and biomass fractionation. This study investigates the effects of ChCl:LA (1:2) DES pretreatment under varying temperatures (100–140 °C) and reaction times (3-6 h) on the chemical composition, structural modification, delignification kinetics, and enzymatic digestibility of OPEFB. A modified combined delignification factor (CDF) was developed to unify temperature, time, and DES acidity into a single severity descriptor. Delignification followed a biphasic pattern successfully captured by the CDF-based kinetic model ($R^2 = 0.9961$), with activation energy of 63.5 kJ.mol^{-1}. Increasing pretreatment severity enhanced hemicellulose and lignin removal (up to 95.5% and 84.4%), while cellulose remained largely preserved. SEM, XRD, and FTIR analyses confirmed progressive disruption of the lignin–carbohydrate matrix, increased cellulose exposure, and removal of amorphous domains. As a result, enzymatic hydrolysis yield improved by more than twofold relative to untreated biomass, reaching 75.5% at 140 °C for 6 h. Mass-balance evaluation demonstrated that from 100 g OPEFB, DES pretreatment yielded 21.6 g glucose and 24.7 g recoverable lignin under optimal conditions. Compared to other pretreatment strategies, the ChCl:LA DES system achieved a balanced co-production of sugars and lignin in significantly shorter processing time. Overall, this work provides mechanistic, kinetic, and mass-balance insights into DES-assisted fractionation of OPEFB and highlights its potential in integrated multiproduct biorefineries.

Keywords: Oil palm empty fruit bunch; deep eutectic solvent; fractionation; enzymatic hydrolysis; severity factor

How to Cite: Wijaya, C., Pertiwi, U. N. L., Apol, T. R., Rohmah, I. P. N., Muharja, M., Widjaja, T., Riadi, L., Widjaja, A. (2026). Enhancing Enzymatic Digestibility and Lignin Production of Oil Palm Empty Fruit Bunch (OPEFB) by Green Deep Eutectic Solvent. *Bulletin of Chemical Reaction Engineering & Catalysis*, 21 (2), 412-427. (DOI: 10.9767/bcrec.20526)

Permalink/DOI: https://doi.org/10.9767/bcrec.20526

1. Introduction

The world is facing severe challenges from climate change and environmental degradation caused by excessive fossil-fuel consumption. Developing renewable and sustainable feedstocks for the production of fuels, chemicals, and biomaterials has therefore become an urgent global priority [1,2]. Lignocellulosic biomass represents a promising renewable resource for biorefineries because of its abundance, carbon neutrality, and potential to generate a broad range of value-added bioproducts and biofuels [3–7]. However, its rigid cell-wall architecture, composed mainly of cellulose, hemicellulose, and lignin tightly bound through lignin–carbohydrate linkages, limits enzymatic hydrolysis and efficient conversion [8]. Accordingly, the establishment of an effective pretreatment process to overcome this

---

* Corresponding Author.
Email: arief.widjaja@its.ac.id (A. Widjaja)

recalcitrance has become a critical step in the valorization of lignocellulosic biomass [9,10].

Oil-palm empty fruit bunch (OPEFB) is one of the most abundant agricultural residues generated in tropical regions, particularly in Indonesia. In 2019, the production of OPEFB was approximately 45.86 Mt per year, accounting for about 75.7% of the global supply [11]. The expanding global demand for crude palm oil (CPO) has led to a continuous increase in OPEFB accumulation. Despite its high annual output, OPEFB is still utilized mainly as a low-value material for mulching or combustion, which cannot compensate for the associated environmental burden. As a lignin-rich feedstock containing roughly 35–45 % cellulose, 25–30 % hemicellulose, and 25–30 % lignin [12], OPEFB possesses great potential for bioconversion into fermentable sugars, biochemicals, and functional materials. However, its high lignin content and compact fiber structure require an efficient fractionation strategy to unlock its biorefinery potential [13].

Various physical, chemical, and physicochemical pretreatment technologies have been developed to fractionate lignocellulosic biomass, including dilute-acid hydrolysis, alkaline delignification, organosolv, and hydrothermal pretreatment [14–19]; however, these conventional approaches often suffer from high energy demand, equipment corrosion, and limited selectivity for lignin removal. In recent years, deep eutectic solvents (DESs) have emerged as green and tunable alternatives capable of selectively dissolving lignin while preserving cellulose integrity [20–22]. DESs are formed via hydrogen-bond interactions between a hydrogen-bond acceptor (HBA) and hydrogen-bond donor (HBD), producing low-volatility, low-toxicity, and recyclable solvent systems [23,24]. Among them, choline chloride (ChCl)-based DESs incorporating organic acids such as lactic acid (LA) have demonstrated superior delignification efficiency and strong compatibility with enzymatic hydrolysis [25,26]. Comparative studies indicate that ChCl:LA can achieve delignification up to 94.4–95% at 120 °C (3–6 h) with cellulose recovery around 91% [27], and enzymatic glucan hydrolysis of approximately 92.7% after mild pretreatment (120 °C, 1 h), although performance may decline upon repeated cycles without solvent refreshing [28]. In contrast, ChCl:urea and ChCl:glycerol systems tend to favor fiber defibrillation rather than lignin extraction under conditions such as 140 °C for 6 h (1:2 mol ratio), resulting in lower lignin removal and reduced glucan conversion (up to 72.6%), despite good enzyme stability in the case of ChCl:glycerol [29]. Acidic HBDs such as formic or oxalic acids show matrix-dependent performance without consistently surpassing ChCl:LA [30,31], while ChCl:levulinic systems remain promising but lack standardized comparative metrics [32,33]. Additionally, cost and feedstock availability favor ChCl:LA due to the scalability of ChCl and lactic acid and reported process-level cost reductions [32,34]. Mechanistically, ChCl provides strong hydrogen-bonding capacity and ionic character, whereas lactic acid introduces mild acidity that facilitates cleavage of ether and ester linkages within the lignin–carbohydrate complex (LCC), supporting efficient fractionation [35–37]. Accordingly, ChCl:LA-based DES pretreatment is widely regarded as an environmentally benign and effective strategy for lignocellulosic biomass fractionation.

Although numerous studies have demonstrated the ability of ChCl-based DESs to dissolve lignin and improve enzymatic digestibility, a mechanistic understanding of how pretreatment intensity influences the selective fractionation of OPEFB remains limited [38,39]. Moreover, most previous works emphasized sugar yield enhancement, whereas the structural evolution and potential valorization of the lignin fraction received less attention [40,41]. To address these gaps, pretreatment severity indices have been introduced to quantify process intensity and correlate it with biomass deconstruction. Traditionally, the overall severity of hydrothermal reactions is expressed by the logarithmic severity factor, which combines temperature and reaction time [42,43]. However, this empirical parameter neglects solvent composition and catalytic effects, which are critical in non-aqueous or hybrid solvent systems. Recently, a modified severity factor, termed the combined delignification factor (CDF), has been developed to provide a more comprehensive evaluation of lignin removal kinetics under variable reaction conditions [44,45]. These modified parameters enable a more accurate description of process severity in DES pretreatment.

The present study investigates a DES pretreatment strategy for OPEFB using a ChCl:LA system under various severity conditions. It was hypothesized that the synergistic action of thermal activation and the hydrogen-bond network in ChCl:LA would effectively disrupt the LCC structure, enhance hemicellulose solubilization, and promote lignin extraction while preserving cellulose. Accordingly, this work aimed to (i) evaluate the effect of operational conditions on the chemical composition and component removal of pretreated OPEFB, (ii) model delignification using CDF as modified severity parameters, and (iii) examine the relationship between pretreatment conditions, lignin characteristics, and enzymatic hydrolysis efficiency. The results provide a comprehensive understanding of OPEFB fractionation under relatively mild operating conditions conditions and establish a foundation for its biorefinery conversion into fermentable sugars and functional lignin-derived materials.

2. Materials and Methods

2.1 Materials

OPEFB was obtained from PT. Sawit Arum Madani, Blitar, Indonesia. The biomass was washed and prepared according to NREL Protocol [45], and subsequently milled to achieve a particle size of 40–60 mesh. L(+)-lactic acid and choline chloride, used as the constituents of the deep eutectic solvent (DES), were purchased from Merck (Germany) and Sigma-Aldrich (USA), respectively. The cellulase enzyme from *Trichoderma reesei* and all other analytical-grade reagents were supplied by Sigma-Aldrich (USA).

2.2. DES Preparation and Pretreatment of OPEFB Biomass

The steps of DES preparation and pretreatment were adapted from a previous study [46]. The DES was prepared by combining lactic acid and choline chloride at a molar ratio of 2:1, followed by heating in a closed round-bottom flask at 70 °C with continuous stirring until a clear and homogeneous liquid was obtained. The mixture was subsequently cooled to room temperature prior to use. For DES pretreatment, 3 g of OPEFB was mixed with 60 g of DES in a 250 mL three-neck round-bottom flask. The pretreatment was carried out at 120–140 °C for 3–6 h [47]. Upon completion, 60 mL of ethanol was added to the slurry, followed by vacuum filtration. The residual solids were washed with an ethanol–water mixture and subsequently dried in an oven at 60 °C prior to further analysis. The lignin-rich DES fraction was further processed for lignin recovery [48]. Deionized water was added to the filtrate at a ratio of 1:5 (filtrate:water) to induce lignin precipitation. The precipitated lignin was separated by centrifugation (HERMLE Z306 universal centrifuge) at 10,000 rpm for 10 min and dried in an oven at 60 °C before characterization.

The removal of lignin was modeled according to a modified severity factor that could unify the pretreatment operation conditions such as temperature, time, and concentration of DES during pretreatment. The removal of lignin from OPEFB, based on its depolymerization behavior, was described by the following equations:

$$\frac{dL_{res}}{dt} = -k(T, C, \ldots)CL_{res} \quad (1)$$

where L_{res} represents the residual content component of lignin and remained in the pretreated solid, while T is the reaction temperature (K), C denotes the lactic acid concentration (mol/L) in DES system. The reaction rate constant, $k(T, C, \ldots)$ is a function of temperature, lactic acid concentration in this study, and other influencing factors. The rate constant (k) was expressed using an Arrhenius-type formulation that incorporates the catalytic effect of DES system, as shown in [49,50]:

$$k = \exp\left(\alpha - \frac{E_a}{RT} + \beta C\right) \quad (2)$$

where E_a denotes the apparent activation energy (J/mol), R is the universal gas constant (8.314 J/mol·K), and α and β are empirically fitted parameters.

Lignin was assumed to consist of two distinct fractions: fast-reacting (L_f) and slow-reacting (L_s) components. The hydrolysis kinetics of each fraction were described by the following rate equations, as shown in Equations (3) and (4) [44,49,50]:

$$\frac{dL_f}{dt} = -kCL_f \quad (3)$$

$$\frac{dL_s}{dt} = -fkCL_s \quad (4)$$

where, f represents the ratio of the rate constants for slow- and fast-reacting lignin, while θ denotes the initial fraction of slow-reacting fraction. The equations presented are analogous to previous research on the Lewis acid hydrolysis of xylan during hydrothermal pretreatment, which identified both slow and fast hydrolyzing components of xylan [45]. Moreover, as pretreatment is influenced by factors such as temperature, duration, and catalytic agents, a similar approach is applied during DES pretreatment to correlate with lignin dissolution. By solving the corresponding differential equations, the residual content can be represented as a function of the modified severity factor, a combined delignification factor (CDF) for the delignification of OPEFB, which is analogous to the combined hydrolysis factor (CHF) identified in previous research during xylan hydrolysis. Based on this formulation, the CDF for a given reaction time t was defined as shown in Equation (5).

$$CDF = \exp\left(\alpha - \frac{E_a}{RT} + \beta C\right)Ct \quad (5)$$

Equations (3) and (4) were solved to yield Equation (6):

$$L_{res} = (1 - \theta)\exp(-CDF) + \theta\exp(-fCDF) \quad (6)$$

The model was fitted to the experimental data to estimate the kinetic parameters α, β, E_a, θ, and f, thereby elucidating the effects of pretreatment conditions, particularly temperature and LA concentration, on delignification, and overall pretreatment performance. The objective function

F was minimized to achieve the best fit between the predicted and experimental values of residual component of interest, as described as follow:

$$F = \sum_{i=1}^{N} \left(X_{\text{res}}^{\text{model}} - X_{\text{res}}^{\text{exp}}\right)^2 \tag{7}$$

where, N is the number of data points, $X_{\text{res}}^{\text{model}}$ and $X_{\text{res}}^{\text{exp}}$ are the modeled and experimental residual lignin respectively. This objective function was minimized using MATLAB 2025a.

2.3. Enzymatic Hydrolysis of Pretreated OPEFB

Enzymatic hydrolysis or saccharification of the pretreated OPEFB residue samples was carried out in an Erlenmeyer flask with 0.5 g of biomass, 0.05 M sodium citrate buffer (pH of 4.8), and cellulase enzyme at 17.5 FPU/biomass (g). The Erlenmeyer flask was incubated in an incubator shaker (50 °C, 150 rpm) for 72 hours. The saccharification yield was calculated using Equation (8) as follows:

$$Y_{EH} = \frac{glucose \times 0.9\ (gram)}{cellulose\ in\ OPEFB\ (gram)} \times 100\% \tag{8}$$

2.4. Compositional Analysis of Pretreated OPEFB and Enzymatic Hydrolysate

To assess sugar content, hydrolysates from both solid compositional hydrolysate and enzymatic hydrolysis processes were examined using high-performance liquid chromatography (HPLC). The analysis employed a Thermo Scientific Vanquish Core HPLC (Thermo Scientific, USA) with a HyperREZ XP Carbohydrate Pb++ column (8 µm, 300×7.7 mm) (Thermo Scientific, USA) and a refractive index (RI) detector. The HPLC was operated under the following conditions: a flow rate of 0.6 mL/min, a temperature of 85 °C, a pressure of 9 bar, and HPLC-grade water served as the mobile phase.

The biomass was analyzed compositionally using the NREL method [45]. This approach entailed hydrolyzing the biomass with concentrated sulfuric acid to measure the carbohydrate components (monomeric sugars) and to assess the lignin content, which includes both acid-soluble lignin (ASL) and acid-insoluble lignin (AIL).

The evaluation of DES pretreatment's effect on OPEFB biomass was conducted. The extent to which specific components of OPEFB were removed was determined using Equation (9).

$$R_i(\%) = \left(1 - \frac{pretreated\ OPEFB\ component\ mass_{(g)}}{initial\ OPEFB\ component\ mass_{(g)}}\right) \times 100 \tag{9}$$

where, R_i represents the removal percentage of a specific OPEFB component i (hemicellulose, cellulose, or lignin). Meanwhile the recovered lignin (Y_L) for each pretreatment was calculated as follows:

$$Y_L = \frac{Isolated\ lignin\ (gram)}{Lignin\ from\ OPEFB\ (gram)} \times 100\% \tag{10}$$

2.5. Morphology, Functional Group, and Crystallinity Analyses of OPEFB

The study examined how pretreatment variables affect crystalline, morphology, and functional groups of OPEFB. The crystallinity of both DES-treated and untreated OPEFB solid fractions was assessed using X-ray diffraction (XRD) in accordance with Segal's method [51]. XRD analysis was conducted with an X'Pert PRO (PAN-analytical BV, Netherlands), utilizing Cu Kα radiation at 40 kV and 30 mA. The crystallinity index (CrI) was determined using Equation (11).

$$CrI\ (\%) = \frac{I_{002} - I_{am}}{I_{002}} \times 100\% \tag{11}$$

where I_{002} denotes the intensity of the 002 cellulose diffraction plane at 22.6°, and I_{am} signifies the intensity of the amorphous cellulose region at 18°.

To investigate morphological alterations in OPEFB after different pretreatments, scanning electron microscopy (SEM) (Hitachi FlexSEM 1000, Japan) was utilized. Furthermore, Fourier transform infrared (FTIR) spectroscopy (Agilent Cary 630 FTIR Spectrometer, USA) was used to evaluate changes in the functional groups of the OPEFB samples.

2.6. Lignin Characterizations

Fourier Transform Infrared (FTIR) spectroscopy was employed to investigate alterations in the chemical structure of Oil Palm Empty Fruit Bunch (OPEFB) using a PerkinElmer System 2000 FTIR, spanning a spectral range from 4000 to 650 cm^{-1}. The FTIR measurements were performed in transmission mode. For comparative analysis with other pretreatment methods, organosolv lignin was selected. The procedure for obtaining organosolv lignin is as follows [52]: pretreated OPEFB solid was combined with aqueous ethanol at varying concentrations, maintaining a solid-to-liquid ratio of 1:10. The reaction was conducted at 180°C with 80% EtOH for 60 minutes and maintained for 30 minutes. Subsequently, the reactor was cooled to 30°C, and the suspension was filtered to separate the solid phase containing cellulose from the liquid phase containing lignin. The solid OPEFB was washed with ethanol at 70 °C and 50 wt%. It was then rinsed three times with water to remove any residual ethanol. The solid OPEFB was dried in an oven at 60 °C until a constant weight was achieved. The washing liquid, comprising lignin and ethanol solvent, was allowed to precipitate at 4 °C overnight. It was then subjected to centrifugation at 10,000 rpm for 15 minutes. The resulting lignin solid was subsequently oven-dried at 60 °C.

2.7. Statistical Analysis

The nonlinear regression model (Equation (6)) that characterizes delignification underwent a statistical evaluation. Parameters of the model (α, E_a, β, θ, and *f*) were determined through nonlinear least-squares fitting, and their significance was tested using t-tests at a 95% confidence interval. For each parameter, both the estimated value and the p-value were documented. The model's overall fit quality was assessed using R^2, while the statistical validity of the model was confirmed through ANOVA of the regression (F-test). All analyses were conducted using MATLAB R2025a.

3. Results and Discussion

3.1 Effect of DES pretreatment conditions on OPEFB composition and lignin removal

Figure 1 presents the effects of DES pretreatment on the removal of lignocellulosic components and the subsequent changes in the solid composition of OPEFB under various temperature and reaction time conditions. Figure 1a illustrates the removal percentages of hemicellulose, lignin, cellulose, and the yield of successfully isolated lignin, while Figure 1b shows the impact of these removals on the relative proportions of cellulose, hemicellulose, and lignin remaining in the pretreated solids. Hemicellulose removal (R_H) increased consistently with both temperature and reaction time. At 100 °C, hemicellulose removal was moderate (65.82%), reflecting limited solubilization under mild conditions. As temperature increased to 120 °C and 140 °C, hemicellulose removal became more pronounced (up to 93.75%), particularly at 6 h. This suggests that DES efficiently breaks the ester and ether bonds in hemicellulose when subjected to higher thermal energy and as the process continues over time [53]. This trend aligns with the known susceptibility of hemicellulose, an amorphous and thermally labile polysaccharide, to dissolution in acidic or hydrogen-bonding DES systems [8]. Moreover, the mass transfer during pretreatment is enhanced by reducing the viscosity of the solution at elevated temperatures, thereby facilitating the mass transfer processes during extraction. These phenomena have been corroborated by other studies, which indicate that at higher temperatures, the removal of hemicellulose is similarly increased. Specifically, when the temperature is raised from 100 °C to 140 °C, hemicellulose removal in maleic acid-polyethylene glycol-choline chloride systems increases from 72% to 93% [54].

Meanwhile, the removal of lignin (R_L) demonstrated a similar enhancement dependent on both temperature and time. At 100 °C at 3 h, lignin removal was limited (38.2%), indicating a partial disruption of lignin–carbohydrate complexes. However, increasing the temperature to 120 °C, and particularly to 140 °C, resulted in significantly higher lignin removal, with the most substantial delignification observed at 140 °C for a duration of 6 hours (84.4%). The decrease in lignin proportion in the solids also correlates with the increased lignin yield in the liquid phase, confirming that the lignin removed from the biomass matrix is being effectively extracted by DES [55]. This delignification improvement can be attributed to the enhanced interactions between DES and lignin functional groups. The ChCl, serving as the HBA, and LA, acting as the HBD, form a network of hydrogen bonds with the phenolic hydroxyl groups in lignin, thereby facilitating the dissolution of the lignin fraction [56]. Furthermore, the acidic nature of the HBD in this system (LA) possesses protons that can

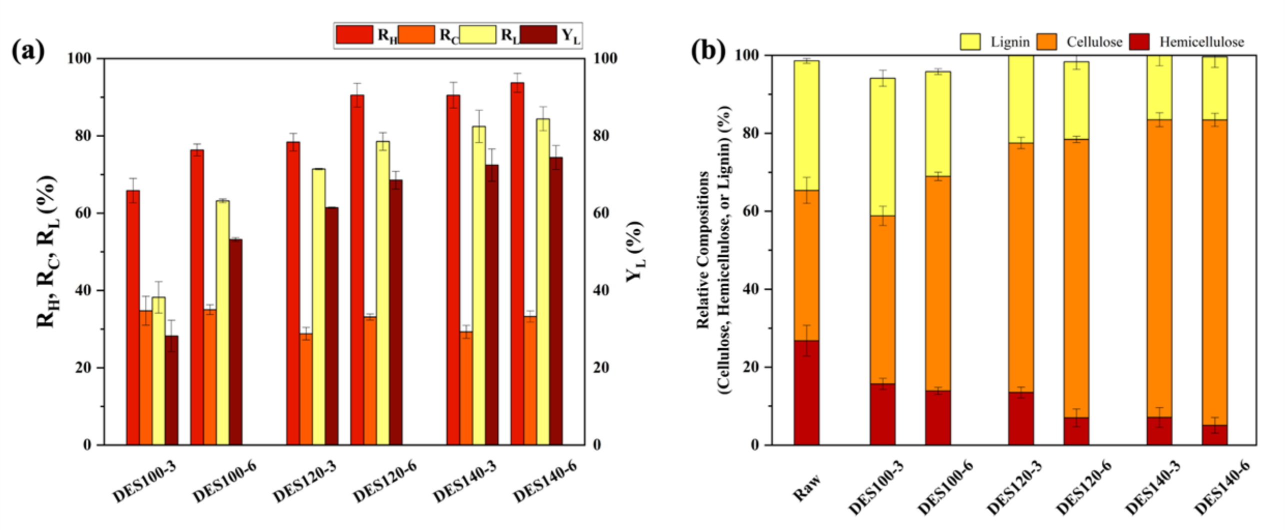

Figure 1. Effect of DES pretreatment conditions on lignin yield, component removals (a) and relative compositions (b) of OPEFB.

catalyze the cleavage of β–O–4 linkages within the lignin structure, a process that becomes more efficient at elevated temperatures [57]. Similar to the dissolution of hemicellulose, once the lignin fraction is depolymerized through the aforementioned mechanism, the mass transfer of lignin extraction is enhanced during pretreatment at higher temperatures [58]. Similar phenomena have been observed in other research, which reported that lignin removal increased with higher temperatures, specifically from 90 °C to 130 °C, resulting in delignification levels rising from 33% to 77% in lactic acid-betaine hydrochloride [59].

In contrast to hemicellulose and lignin, cellulose removal (R_C) remained consistently low across all pretreatment conditions (<35.1%). This behavior reflects the intrinsic recalcitrance of cellulose, whose crystalline regions and strong hydrogen-bonding network are not easily disrupted by DES [60]. The low cellulose removal is advantageous because it preserves the structural integrity of cellulose in the solid fraction, making it a suitable substrate for downstream enzymatic hydrolysis or further processing [61].

The component removals in Figure 1a correspond directly to the compositional shifts observed in Figure 1b. As hemicellulose and lignin are progressively removed, their proportions in the solid decrease, causing the relative cellulose content to increase. This enrichment effect becomes most pronounced at 140 °C, where delignification and hemicellulose dissolution are maximal in this study. The remaining solids at these conditions contain a substantially higher proportion of cellulose and significantly reduced lignin content, reflecting successful disruption of lignin–carbohydrate complexes and selective solubilization of non-cellulosic components [22]. Overall, the pretreatment with deep eutectic solvents (DES) exhibits a distinct selective fractionation pattern, hemicellulose is initially and most readily removed, lignin dissolution significantly increases with both temperature and duration, while cellulose remains largely unaffected. These removal behaviors directly influence the composition of the pretreated solids and determine the lignin yield in the liquid fraction. The strong correlation between increased pretreatment variables, higher lignin removal, and elevated lignin yield underscores the efficacy of DES as a delignification medium.

3.2. CDF-based Modeling and Kinetic Interpretation of OPEFB Delignification during DES Pretreatment

The observed trend of increased lignin removal with rising temperature and extended time, as illustrated in Figure 1, can be modeled to assess the effect of a unified parameter. This parameter represents the combined influence of temperature, time, and the constituents of DES, as demonstrated in Figure 2. Figure 2 illustrates the correlation between the CDF, a unified parameter encompassing temperature, time, and DES constituent, and the residual lignin fraction (L_{res}) as the response. It also includes a parity plot that compares model-predicted values with those obtained experimentally. The trend depicted in Figure 2a demonstrates a rapid decrease in (L_{res}) at low CDF values, followed by a gradual approach toward a lower asymptotic limit as CDF increases. This pattern indicates that lignin removal is highly sensitive to initial increases in pretreatment severity, during which readily cleavable lignin–carbohydrate linkages and amorphous lignin domains are rapidly solubilized. Beyond a CDF of approximately 4–5, the curve begins to plateau, suggesting that the remaining lignin becomes increasingly resistant

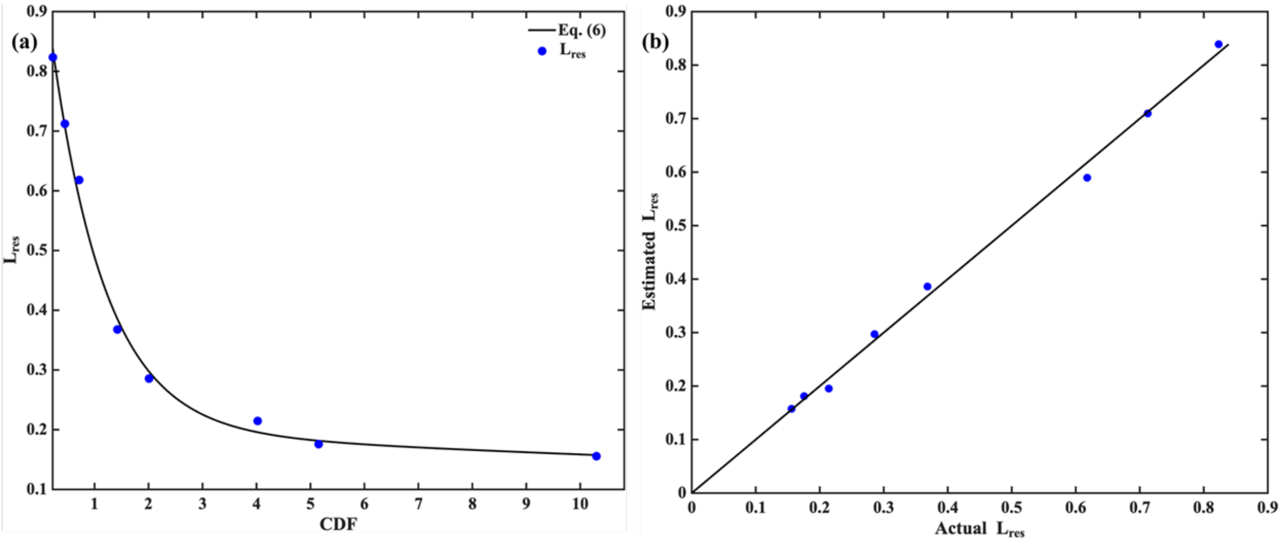

Figure 2. (a) Relationship between CDF and L_{res}, as modeled by Equation (6); (b) Parity plot comparing actual and predicted values of L_{res}.

to degradation due to its more crosslinked, structurally stable nature, and higher diffusion resistance as it penetrates deeper into the cell wall, and forming a condensed structure at higher temperature [58,62]. The fitted curve based on Equation (6) accurately captures this biphasic delignification profile, reflecting the combined kinetic contributions of temperature and solvent-driven delignification. The close match between the model and data points ($R^2 = 0.9961$) indicates that the CDF formulation effectively represents the severity-dependent behavior of lignin removal during pretreatment. This rapid-to-slow transition in L_{res} aligns with the typical two-stage delignification kinetics observed in lignocellulosic biomass, where easily accessible lignin is removed quickly, while residual lignin requires higher severity or prolonged exposure for further depolymerization [63,64].

The fitted kinetic parameters obtained from the model are summarized in Table 1. Among the parameters, the activation energy (E_a) exhibited a strongly significant effect (F = 161.55, p = 0.0011), confirming that temperature plays a dominant role in controlling lignin solubilization. The fitted value of 63.5 kJ/mol is consistent with reported activation energies for lignin depolymerization in various pretreatment systems, further supporting the physical relevance of the model. The parameter θ (0.199) was also statistically significant (F = 14.174, p = 0.0328), indicating that it contributes meaningfully to capturing the curvature of the CDF – L_{res} relationship, particularly the transition from the rapid initial degradation phase to the slower delignification regime. The activation energy (E_a) of 63.5 kJ/mol is notably lower than the value of 95.8 kJ/mol reported in another study involving the p-toluenesulfonic acid (p-TsOH) system. This indicates that the ChCl:LA DES system exhibits a reduced activation energy, thereby enhancing its efficacy in the delignification of lignocellulose biomass [44]. Besides, (f, α, and β) showed limited statistical significance ($p > 0.05$), implying that their influence on L_{res} is less pronounced within the experimental range studied. Their inclusion, however, contributes to fine-tuning the model across the entire CDF domain and may hold greater relevance under broader operational conditions not represented in the current dataset. Their low F-values suggest that variations in these secondary factors do not substantially impact lignin removal compared to the dominant effects captured by E_a and θ. The predictive capability of the fitted model is validated by the parity plot shown in Figure 2b. The close alignment of data points along the 1:1 line indicates strong agreement between the estimated and experimental L_{res} values across all pretreatment conditions. This demonstrates that the CDF-based model provides both a statistically reliable and mechanistically meaningful framework for describing lignin degradation behavior. The results indicate that the development of the CDF serves as a predictive tool for correlating operational variables with the extent of delignification. Moreover, it can be utilized as a scale-up parameter in industrial applications, as it effectively captures the primary controlling variables during the delignification of biomass [45].

Table 1. CDF modelling parameters and ANOVA result.

Model Parameters	Unit	Fitted Value	F-value	p-value
E_a	kJ/mol	63.5	161.55	0.0011
θ	none	0.199	14.174	0.0328
f	none	0.022	0.4700	0.5422
α	none	2.71	0.0016	0.9709
β	L/mol	3.12	0.0257	0.8828

3.3. Physicochemical and Structural Characterization of DES-pretreated OPEFB and Recovered Lignin

The morphological, structural, and chemical transformations of OPEFB following DES pretreatment at 100–140 °C for 6 hours were examined using SEM, XRD, and FTIR analyses (Figure 3). These analytical techniques offer complementary insights into the extent of biomass disruption, alterations in functional groups, and variations in cellulose crystallinity, all of which are essential for comprehending the fractionation behavior induced by DES.

The SEM micrographs presented in Figure 3a illustrate a distinct progression of morphological disruption as the pretreatment temperature increases. The untreated OPEFB fibers display a compact and rigid surface with minimal visible porosity, indicative of the intact lignin–hemicellulose network that securely binds the cellulose microfibrils. Following pretreatment at 100 °C, there is evidence of partial surface peeling and loosening of the fiber bundles, suggesting initial solubilization of hemicellulose and partial delignification. At 120 °C, the fibers exhibit increased separation and a rougher surface, consistent with the enhanced removal of hemicellulose and the weakening of lignin–carbohydrate complexes. The most extensive structural disintegration is observed at 140 °C, where the fibers show significant fibrillation, cracks, and exposed cellulose microfibrils. This pronounced disruption aligns with the highest lignin and hemicellulose removal observed in Figure 1, confirming that DES effectively penetrates and deconstructs the biomass matrix. The increased surface roughness and fiber separation at elevated temperatures also suggest improved accessibility to cellulose, which is advantageous for subsequent hydrolysis or functionalization processes [65].

The crystallographic properties of DES-pretreated OPEFB were evaluated using XRD (Figure 3b). The CrI values demonstrate a clear dependence on the pretreatment temperature. The untreated biomass exhibits a CrI of 65.6%, which increases to 80.8%-82% following treatment at 100-140 °C. This enhancement in crystallinity confirms the preferential removal of amorphous components, primarily hemicellulose and portions of amorphous lignin, resulting in the relative enrichment of crystalline cellulose [65]. Such behavior is characteristic of DES pretreatment, where selective solubilization of non-crystalline domains enhances the overall ordering of the cellulose fraction. However, at the higher temperature of 140 °C, the CrI remains relatively constant at approximately 81.0%, indicating the onset of partial cellulose disruption or disordering at elevated temperatures, even though the composition of cellulose is highest at 140°C and 6 hours. This suggests that although DES is selective, excessive severity may begin to erode crystalline cellulose or increase fiber swelling to the extent that crystallinity appears reduced [66].

FTIR analysis (Figure 3c and Table 2) provides further insight into the chemical modifications induced by DES pretreatment. The broad O–H stretching band observed around 3300–3400 cm^{-1} exhibits a decrease in intensity post-pretreatment, indicating the disruption of intermolecular hydrogen bonding and the partial dissolution of lignin and hemicellulose [67]. The peak near 2907 cm^{-1}, associated with C–H stretching in lignin aliphatic groups, diminishes with increasing temperature, reflecting progressive delignification [68]. A significant reduction in the ester carbonyl peak around 1729 cm^{-1} confirms the removal of hemicellulose, as this region corresponds to acetyl and uronic ester groups prevalent in hemicellulosic structures [69]. Furthermore, the aromatic skeletal vibrations at 1600–1510 cm^{-1} show reduced intensity, consistent with lignin solubilization and modification during DES pretreatment [47].

Table 2. FTIR peak spectrum and corresponding functional group.

Peak (cm^{-1})	Functional Group	References
3333	Interactions (-OH) involving hydrogen bonds occur both within and among the molecules of hemicellulose, cellulose, and lignin.	[68]
2907	Aliphatic C-H stretching in lignin.	[68]
1729	Carbonyl ester groups (C=O) in lignin or acetyl groups in hemicelluloses.	[69].
1603	Aromatic ring (C=C) stretching vibrations characteristic of lignin.	[47]
1509	Additional aromatic ring stretching vibrations observed in lignin.	[47]
1371	C-H, O-H, or C-O bonds, commonly found in hemicelluloses.	[47,70]
1327	C-H, O-H, or C-O bond vibrations associated with hemicelluloses.	[47,70]
1238	Stretching of C-H, O-H, or C-O bonds in hemicelluloses.	[47,70]

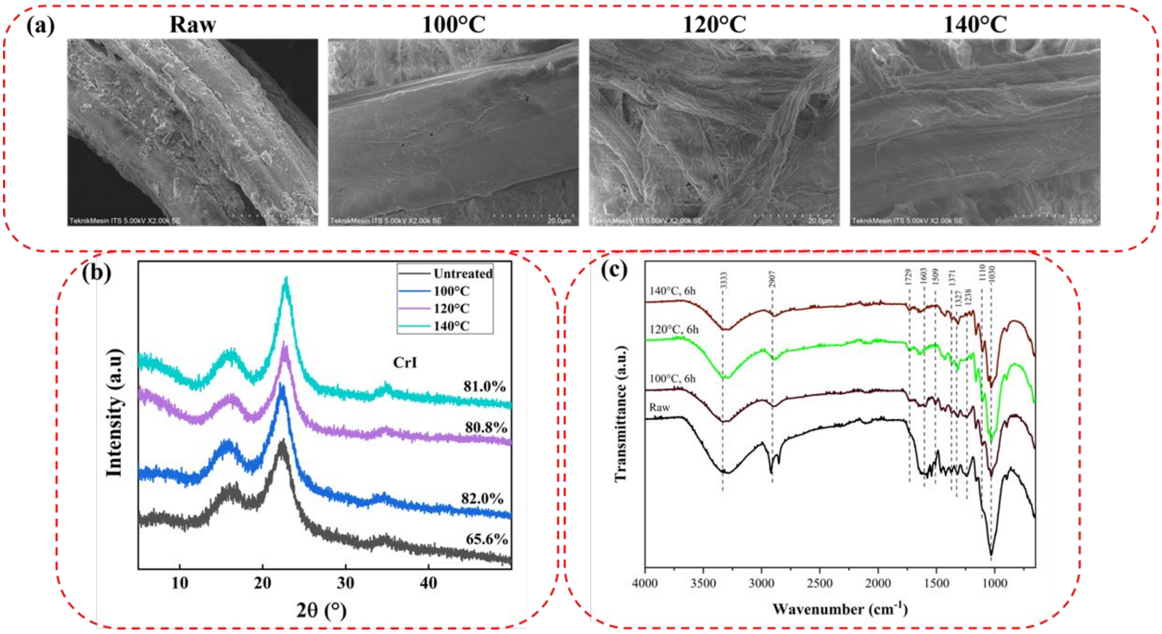

Figure 3. SEM, XRD, and FTIR of pretreated OPEFB (100-140 °C, 6 h).

Peaks associated with hemicellulose, such as those near 1371 cm⁻¹ (C–H bending) and 1238 cm⁻¹ (C–O stretching) also weaken or shift, reflecting the progressive cleavage of hemicellulosic linkages [47,70]. Collectively, the FTIR spectrum confirms selective fractionation, with DES effectively removing hemicellulose and modifying lignin while largely preserving cellulose functional groups.

The combined results from SEM, XRD, and FTIR analyses indicate that DES pretreatment substantially modifies the physicochemical and structural characteristics of OPEFB. An increase in temperature facilitates the removal of amorphous hemicellulose and lignin, resulting in noticeable structure disruption, enhanced cellulose exposure, and increased crystallinity under moderate conditions. These structural and chemical changes align with the fractionation patterns observed in Section 3.1 and corroborate the mechanism by which DES selectively dissolves lignin-rich and hemicellulosic domains [8,58]. The enhanced accessibility of cellulose and the altered lignin environment underscore the potential of DES pretreatment as an effective strategy for biomass deconstruction, lignin recovery, and the valorization of cellulose-rich solids for subsequent processing.

Comparative FTIR analysis between DES-derived lignin and organosolv lignin (Figure 4) revealed both similarities and subtle differences in structural features. Both samples exhibited broad O–H stretching bands in the 3315 cm⁻¹ region, confirming the presence of aliphatic and phenolic hydroxyl groups. However, the DES lignin showed a slightly broader and more intense O–H absorption, which may suggest higher hydroxyl availability, potentially associated with cleavage of lignin–carbohydrate linkages during DES treatment. The characteristic aromatic skeletal vibrations at 1606 and 1506 cm⁻¹ were present in both samples, indicating preservation of the aromatic backbone. Notably, the relative intensity of these bands appeared slightly reduced in DES lignin compared to organosolv lignin, which may reflect partial structural modification or differences in condensation behavior under the respective pretreatment conditions. In the 1265–1220 cm⁻¹ region corresponding to guaiacyl and syringyl-associated C–O stretching, both lignins retained characteristic signals, although minor variations in peak sharpness were observed. The absorptions between 1120 and 1030 cm⁻¹, associated with C–O stretching in ether linkages and alcohol groups, remained evident in DES lignin, suggesting that key ether structures were not extensively degraded. Overall, the FTIR comparison indicates that DES pretreatment effectively extracts lignin while largely preserving its aromatic structural framework, with only moderate modification relative to organosolv lignin.

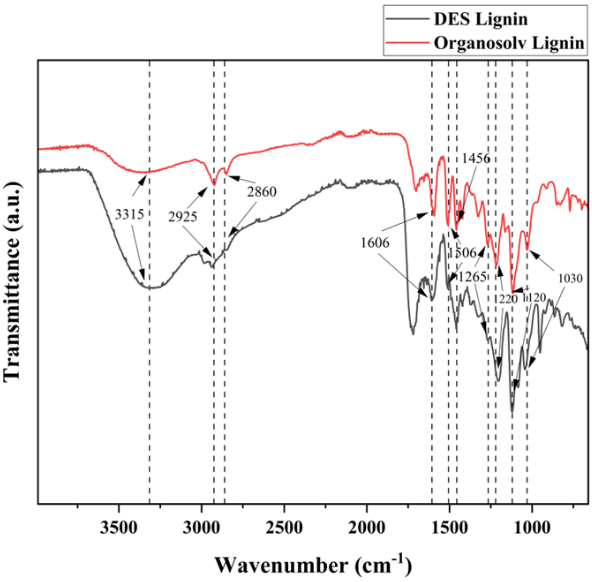

Figure 4. Comparison of OPEFB DES and Organosolv Lignin.

3.4 Enzymatic Hydrolysis Performance of DES-pretreated OPEFB

The enzymatic hydrolysis performance of DES-pretreated OPEFB is depicted in Figure 5. The untreated biomass demonstrated the lowest hydrolysis yield (Y_{EH}), indicative of the inherent recalcitrance of the lignocellulosic matrix, where intact lignin–carbohydrate complexes and limited surface porosity impede enzyme accessibility. Pretreatment at 100 °C significantly enhanced Y_{EH} for both 3-hour and 6-hour durations, increasing the yield by approximately 46.6% and 58.4% compared to the untreated sample. This improvement aligns with the moderate removal of hemicellulose and partial delignification observed previous sections, which begins to expose cellulose

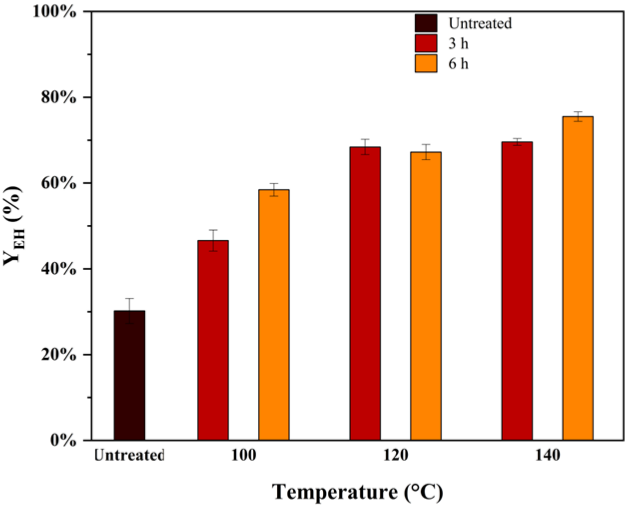

Figure 5. Enzymatic hydrolysis yield (Y_{EH}) of pretreated OPEFB.

microfibrils and weakens the protective lignin barrier. At 120 °C, Y_{EH} exhibited a further increase, surpassing 67.2-68.4% for both pretreatment durations. This notable enhancement can be attributed to the more extensive dissolution of hemicellulose and lignin at this temperature [71], as corroborated by the FTIR and SEM analyses. The FTIR spectra (Figure 3c) reveal clear reductions in hemicellulose-associated peaks (e.g., 1729 cm^{-1} and 1238 cm^{-1}), along with diminished lignin aromatic vibrations, indicating removal of non-cellulose component enhance the cellulose accessibility. SEM images (Figure 3a) display a more disrupted surface with exposed fibrils, which likely facilitates enzyme penetration. XRD results (Figure 3b) also indicate increased crystallinity at moderate temperatures, reflecting the removal of amorphous non-cellulose components that otherwise impede enzymatic activity [16]. Collectively, these structural and chemical changes contribute to the substantial improvement in hydrolysis efficiency observed at 120 °C. The highest enzymatic hydrolysis yields were achieved at 140 °C, with pretreatment durations of 3 hours and 6 hours resulting in Y_{EH} values exceeding 69.6% and approaching 75.5%, respectively. These yields represent more than a twofold enhancement compared to untreated OPEFB. The superior performance at 140°C is consistent with the most extensive lignin and hemicellulose removal observed in previous sections and aligns with the pronounced morphological disruption evident in SEM micrographs. At this level of severity, DES pretreatment effectively removes the majority of the amorphous matrix encasing cellulose, resulting in a highly accessible fiber structure. The highest Y_{EH} values observed at 140 °C, particularly under the 6-hour condition, underscore the strong potential of DES systems for producing cellulose-rich, enzyme-accessible substrates suitable for downstream bioconversion processes.

3.5 Mass-balance Assessment and Comparative Evaluation of DES Pretreatment Efficiency

A detailed mass-balance assessment of DES pretreatment under the selected optimal condition (ChCl:LA, 1:2 at 140 °C for 6 h) is presented in Figure 6. Starting from 100 g of raw OPEFB containing 26.79 g hemicellulose, 38.56 g cellulose, and 33.24 g lignin, the DES pretreatment produced two primary output streams: 32.84 g of solid pretreated OPEFB and 67.16 g of solubilized biomass fraction. This distribution demonstrates the high solubilization capability of the ChCl–lactic acid system, particularly for lignin and hemicellulose. The solid fraction retained after pretreatment contained only 2.98 g hemicellulose, 25.73 g cellulose, and 5.32 g lignin, indicating substantial removal of amorphous polymers. Hemicellulose removal reached 95.5%, consistent with the FTIR evidence of ester bond cleavage and loss of acetyl functionalities [72] (Section 3.3). Lignin removal exceeded 84.4%, confirmed by the weakening of aromatic skeletal bands in FTIR spectra and increased fiber exposure in SEM micrographs [73]. Importantly, cellulose was largely preserved, with 66.7% of the initial cellulose mass retained in the pretreated solid. This selective removal behavior reflects the strong hydrogen-bonding interactions between DES components and lignin/hemicellulose, while crystalline cellulose remains structurally stable under the selected solvent and temperature conditions [74,75]. The solubilized stream comprised 67.16 g of biomass-derived components, including 23.81 g of

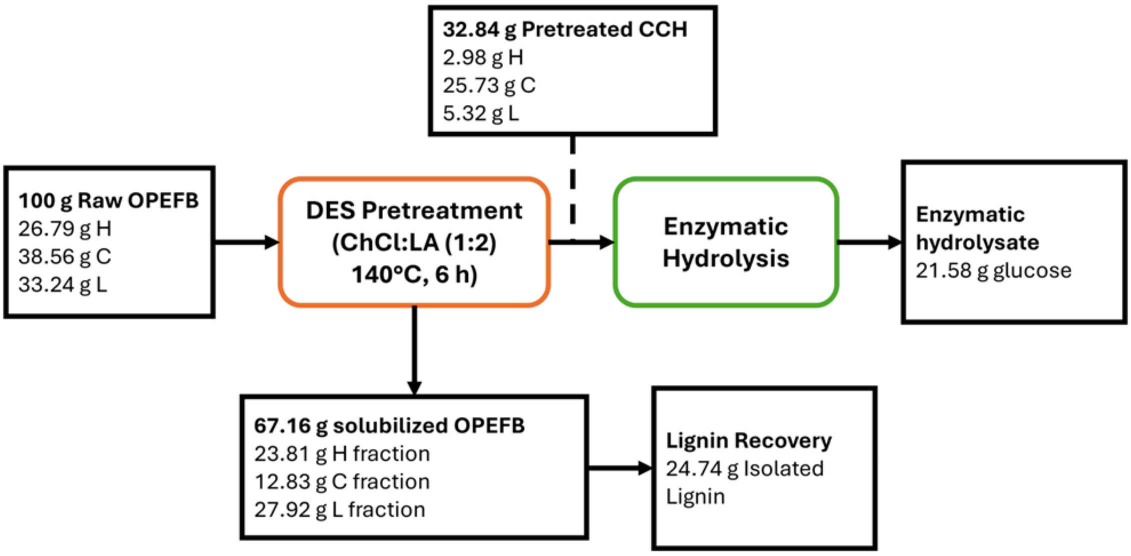

Figure 6. Mass balance of OPEFB DES pretreatment.

hemicellulose, 12.83 g of cellulose-derived soluble fractions, and 27.92 g of lignin. This outcome underscores the significant delignification potential of the ChCl:LA DES system, which effectively disrupts lignin–carbohydrate complexes and solubilizes lignin fragments into the DES phase. Subsequent lignin recovery resulted in 24.74 g of isolated lignin, corresponding to an approximate recovery efficiency of 74.4% relative to the lignin in biomass. The ability to obtain a high-purity lignin stream is advantageous for downstream valorization, such as the production of aromatic monomers or materials applications [76].

Following DES pretreatment, the enzymatic hydrolysis of the cellulose-rich solid yielded 21.58 g of glucose, indicating a significant enhancement in digestibility compared to untreated biomass. The elevated Y_{EH} values reported in Section 3.4 correspond with the substantial removal of lignin and hemicellulose as quantified in this mass balance. By eliminating the non-cellulosic matrix, DES pretreatment increases the accessible cellulose surface area and improves enzyme–substrate interaction, as evidenced by the morphological and crystallinity changes characterized in Section 3.3.

As evidenced by the mass balance analysis, the results were presented and compared with other pretreatment methods in Table 3. Current pretreatment strategies have primarily focused on enhancing glucose yield from enzymatic hydrolysis (EH). The addition of hydrothermal pretreatment using dilute sulfuric acid (H_2SO_4) and maleic acid (MA) resulted in yields of 21.2 grams per 100 grams of OPEFB and 22.3 grams per 100 grams of OPEFB, respectively. Both pretreatments rely on proton catalysis to hydrolyze hemicellulose and disrupt the cellulose structure, thereby increasing enzymatic digestibility [77,78]. However, these methods are unable to extract and isolate lignin from the biomass, as the aqueous base solvent is ineffective in solubilizing lignin. An alternative method, utilizing DES pretreatment composed of ChCl: Oxalic acid (OA) and 20 wt% ethanol, can simultaneously disrupt the cellulose structure and delignify the OPEFB through the HBA and HBD network and protonation of ether bonds, enhancing lignin dissolution [3]. Nevertheless, this result was achieved under impractical operational conditions (80 °C, 24 h), requiring an extended duration to produce 47.9 grams of sugar per 100 grams of OPEFB and yielding a low lignin recovery of 8.8 grams per 100 grams of OPEFB. In contrast, this study demonstrates that ChCl:LA (1:2) at a pretreatment temperature of 140°C for 6 hours can achieve a more balanced outcome in a shorter time, yielding 21.6 grams of sugar per 100 grams of OPEFB and 24.7 grams of lignin per gram of OPEFB. These results contribute to a more diverse product range for a multiproduct biorefinery approach, facilitating the full utilization of biomass [79].

4. Conclusions

This study demonstrates that ChCl:LA deep eutectic solvent pretreatment is an effective strategy for selectively fractionating OPEFB, achieving extensive hemicellulose and lignin removal while preserving cellulose and enhancing enzymatic digestibility. Structural analyses (SEM, FTIR, XRD) confirmed progressive disruption of the lignin–carbohydrate matrix and increased cellulose accessibility, consistent with the improved hydrolysis performance. The unified combined delignification factor (CDF) accurately modeled the biphasic delignification behavior with high reliability ($R^2 = 0.9961$), establishing it as a robust severity index for interpreting DES pretreatment behavior. Under optimal conditions (ChCl:LA 1:2, 140 °C, 6 h), the process achieved 95.5% hemicellulose removal, 84.4% lignin removal, and 75.5% enzymatic hydrolysis yield, producing 21.6 g glucose and 24.7 g isolated lignin per 100 g OPEFB. These findings indicate strong potential for integrating ChCl:LA-based pretreatment into multiproduct biorefinery

Table 3. Previous studies of OPEFB pretreatment. (HT: hydrothermal; DES: deep eutectic solvent; EH: enzymatic hydrolysis; MA: Maleic Acid; EtOh: Ethanol; LA: Lactic Acid; OA: Oxalic Acid)

Process	Conditions	Recovered Lignin (per 100 g raw OPEFB)	EH Glucose (per 100 g raw OPEFB)	Refs.
HT-DA pretreatment & EH	160 °C, 5 h	-	21.2	[77]
HT-MA pretreatment & EH	176.6 °C, 70 min, 1.5% MA	-	22.3	[78]
DES pretreatment & EH	ChCl:OA (1:1) and 20% wt EtOh (80 °C, 24 h) DES: 120 °C, 6 h	8.8	47.9	[3]
DES pretreatment & EH	ChCl:LA (1:2) 140 °C, 6 h	24.7	21.6	This study

schemes by enabling concurrent sugar production and lignin recovery. Although ChCl:LA DES demonstrated high efficiency for selective fractionation and lignin recovery, the recycling and long-term stability of the solvent were not evaluated in this study. Future work should focus on DES recovery efficiency, reuse performance, and solvent stability to assess techno-economic feasibility.

Acknowledgment

This research was financially supported by the Department of Chemical Engineering, Institut Teknologi Sepuluh Nopember, under the Department Research Grant Batch 1, Year 2025 (Contract No. 2398/PKS/ITS/2025, June 3, 2025).

CRedit Author Statement

Author Contributions: PC. Wijaya: Conceptualization, Methodology, Investigation, Data Curation, Writing, Review and Editing; U.N.L. Pertiwi: Investigation, Methodology, Formal Analysis; T.R. Apol: Investigation, Data Curation; I.P.N. Rohmah: Data Curation, Formal Analysis, Visualization; M. Muharja: Supervision, Writing, Review and Editing; T. Widjaja: Supervision, Writing, Review and Editing; L. Riadi: Supervision, Writing, Review and Editing; A. Widjaja: Conceptualization, Supervision, Project Administration, Funding Acquisition, Writing, Review and Editing. All authors have read and agreed to the published version of the manuscript.

References

[1] Bosah, C.P., Li, S., Ampofo, G.K.M., Sangare, I. (2023). A continental and global assessment of the role of energy consumption, total natural resource rent, and economic growth as determinants of carbon emissions. *Science of The Total Environment*, 892, 164592. DOI: 10.1016/J.SCITOTENV.2023.164592.

[2] Chen, X., Yang, H., Zhang, L., Li, Z., Xue, Y., Wang, R., Fan, X., Sun, S. (2023). Green construction and release mechanism of lignin-based double-layer coated urea. *Biotechnology for Biofuels and Bioproducts*, 16(1), 97. DOI: 10.1186/s13068-023-02355-7.

[3] Yong, K.J., Wu, T.Y. (2024). Fractionation of oil palm fronds using ethanol-assisted deep eutectic solvent: Influence of ethanol concentration on enhancing enzymatic saccharification and lignin β-O-4 content. *Environmental Research*, 250, 118366. DOI: 10.1016/J.ENVRES.2024.118366.

[4] Mishra, K., Singh Siwal, S., Kumar Saini, A., Thakur, V.K. (2023). Recent update on gasification and pyrolysis processes of lignocellulosic and algal biomass for hydrogen production. *Fuel*, 332. DOI: 10.1016/j.fuel.2022.126169.

[5] Aline Otaviano, C., Ussemane Mussagy, C., Roberto Paz-Cedeno, F., Fernando Brandão Pereira, J., Masarin, F. (2023). Hydrothermal pretreatment of Eucalyptus by-product and refining of xylooligosaccharides from hemicellulosic hydrolysate. *Separation and Purification Technology*, 306 DOI: 10.1016/j.seppur.2022.122520.

[6] Sutrisna, P.D., Wijaya, C., Robby, C., Liliani, J. (2021). ZIF-8/Cellulose Acetate Based Mixed Matrix Membranes (MMMs) Synthesis and Characterization. In: *Advances in Science and Technology*. Trans Tech Publications Ltd, pp. 57–64. DOI: 10.4028/www.scientific.net/AST.104.57.

[7] Sutrisna, P.D., Hadi, R.P., Wijaya, C., Liliani, J., Robby, C. (2023). Cellulose acetate-Based mixed matrix membrane for methylene blue wastewater treatment. In: *AIP Conference Proceedings*. American Institute of Physics Inc. DOI: 10.1063/5.0112184.

[8] Chen, Z., Wang, Y., Cheng, H., Zhou, H. (2022). Hemicellulose degradation: An overlooked issue in acidic deep eutectic solvents pretreatment of lignocellulosic biomass. *Industrial Crops and Products*, 187, 115335. DOI: 10.1016/J.INDCROP.2022.115335.

[9] Panakkal, E.J., Cheenkachorn, K., Chuetor, S., Tantayotai, P., Raina, N., Cheng, Y.S., Sriariyanun, M. (2022). Optimization of deep eutectic solvent pretreatment for bioethanol production from Napier grass. *Sustainable Energy Technologies and Assessments*, 54, 102856. DOI: 10.1016/J.SETA.2022.102856.

[10] Li, R., Zheng, Y., Zhao, X., Yong, Q., Meng, X., Ragauskas, A., Huang, C. (2023). Recent advances in biomass pretreatment using biphasic solvent systems. *Green Chemistry*, 25(7), 2505–2523. DOI: 10.1039/D3GC00271C.

[11] Suhartini, S., Rohma, N.A., Mardawati, E., Kasbawati, Hidayat, N., Melville, L. (2022). Biorefining of oil palm empty fruit bunches for bioethanol and xylitol production in Indonesia: A review. *Renewable and Sustainable Energy Reviews*, 154, 111817. DOI: 10.1016/j.rser.2021.111817.

[12] Li, M., Jiang, B., Wu, W., Wu, S., Yang, Y., Song, J., Ahmad, M., Jin, Y. (2022). Current understanding and optimization strategies for efficient lignin-enzyme interaction: A review. *International Journal of Biological Macromolecules*, 195, 274–286. DOI: 10.1016/J.IJBIOMAC.2021.11.188.

[13] Gao, H., Wang, Y., Yang, Q., Peng, H., Li, Y., Zhan, D., Wei, H., Lu, H., Bakr, M.M.A., EI-Sheekh, M.M., Qi, Z., Peng, L., Lin, X. (2021). Combined steam explosion and optimized green-liquor pretreatments are effective for complete saccharification to maximize bioethanol production by reducing lignocellulose recalcitrance in one-year-old bamboo. *Renewable Energy*, 175, 1069–1079. DOI: 10.1016/J.RENENE.2021.05.016.

[14] Kininge, M.M., Gogate, P.R. (2022). Intensification of alkaline delignification of sugarcane bagasse using ultrasound assisted approach. *Ultrasonics Sonochemistry*, 82, 105870. DOI: 10.1016/j.ultsonch.2021.105870.

[15] Huang, C., Zhao, X., Zheng, Y., Lin, W., Lai, C., Yong, Q., Ragauskas, A.J., Meng, X. (2022). Revealing the mechanism of surfactant-promoted enzymatic hydrolysis of dilute acid pretreated bamboo. *Bioresource Technology*, 360. DOI: 10.1016/j.biortech.2022.127524.

[16] Su, Y., Wang, P., Lai, C., Huang, C., Ling, Z., Yong, Q. (2023). Revealing key factors influencing enzymatic digestibility of hydrothermally pretreated poplar in comparison with corn stover. *Industrial Crops and Products*, 194. DOI: 10.1016/j.indcrop.2023.116297.

[17] Ovejero-Pérez, A., Rigual, V., Domínguez, J.C., Alonso, M.V., Oliet, M., Rodriguez, F. (2022). Organosolv and ionosolv processes for autohydrolyzed poplar fractionation: Lignin recovery and characterization. *International Journal of Biological Macromolecules*, 197, 131–140. DOI: 10.1016/j.ijbiomac.2021.12.079.

[18] Ahmad, E.F., Lestari, P., Oginawati, K., Yulizar, Y., Sianturi, J., Munir, M.M., Adawiah, A. (2026). Soda-Anthraquinone-Catalyzed Delignification of Coconut Husk Waste. *Bulletin of Chemical Reaction Engineering & Catalysis*, 21(1), 128–136. DOI: 10.9767/bcrec.20537.

[19] Muharja, M., Darmayanti, R.F., Palupi, B., Rahmawati, I., Fachri, B.A., Setiawan, F.A., Amini, H.W., Rizkiana, M.F., Rahmawati, A., Susanti, A., Putri, D.K.Y. (2021). Optimization of microwave-assisted alkali pretreatment for enhancement of delignification process of cocoa pod husk. *Bulletin of Chemical Reaction Engineering & Catalysis*, 16(1), 31-43. DOI: 10.9767/BCREC.16.1.8872.31-43.

[20] Soares, B., da Costa Lopes, A.M., Silvestre, A.J.D., Rodrigues Pinto, P.C., Freire, C.S.R., Coutinho, J.A.P. (2021). Wood delignification with aqueous solutions of deep eutectic solvents. *Industrial Crops and Products*, 160. DOI: 10.1016/j.indcrop.2020.113128.

[21] Majová, V., Jablonský, M., Lelovský, M. (2021). Delignification of unbleached pulp by ternary deep eutectic solvents. *Green Processing and Synthesis*, 10(1), 666–676. DOI: 10.1515/gps-2021-0066.

[22] Yu, H., Xue, Z., Shi, R., Zhou, F., Mu, T. (2022). Lignin dissolution and lignocellulose pretreatment by carboxylic acid based deep eutectic solvents. *Industrial Crops and Products*, 184. DOI: 10.1016/j.indcrop.2022.115049.

[23] Hansen, B.B., Spittle, S., Chen, B., Poe, D., Zhang, Y., Klein, J.M., Horton, A., Adhikari, L., Zelovich, T., Doherty, B.W., Gurkan, B., Maginn, E.J., Ragauskas, A., Dadmun, M., Zawodzinski, T.A., Baker, G.A., Tuckerman, M.E., Savinell, R.F., Sangoro, J.R. (2021). Deep Eutectic Solvents: A Review of Fundamentals and Applications. *Chemical Reviews*, 121(3), 1232–1285. DOI: 10.1021/acs.chemrev.0c00385.

[24] Gabriele, F., Chiarini, M., Germani, R., Tiecco, M., Spreti, N. (2019). Effect of water addition on choline chloride/glycol deep eutectic solvents: Characterization of their structural and physicochemical properties. *Journal of Molecular Liquids*, 291. DOI: 10.1016/j.molliq.2019.111301.

[25] Liang, X., Zhu, Y., Qi, B., Li, S., Luo, J., Wan, Y. (2021). Structure-property-performance relationships of lactic acid-based deep eutectic solvents with different hydrogen bond acceptors for corn stover pretreatment. *Bioresource Technology*, 336(April), 125312. DOI: 10.1016/j.biortech.2021.125312.

[26] Liu, Q., Yuan, T., Fu, Q. jin, Bai, Y. yuan, Peng, F., Yao, C. li (2019). Choline chloride-lactic acid deep eutectic solvent for delignification and nanocellulose production of moso bamboo. *Cellulose*, 26(18), 9447–9462. DOI: 10.1007/s10570-019-02726-0.

[27] Kumar, S., Sharma, S., Arumugam, S.M., Miglani, C., Elumalai, S. (2020). Biphasic Separation Approach in the DES Biomass Fractionation Facilitates Lignin Recovery for Subsequent Valorization to Phenolics. *ACS Sustainable Chemistry & Engineering*, 8(51), 19140–19154. DOI: 10.1021/acssuschemeng.0c07747.

[28] Soleimanzadeh, H., Bektashi, F.M., Ahari, S.Z., Salari, D., Olad, A., Ostadrahimi, A. (2023). Optimization of cellulose extraction process from sugar beet pulp and preparation of its nanofibers with choline chloride–lactic acid deep eutectic solvents. *Biomass Conversion and Biorefinery*, 13(16), 14457–14469. DOI: 10.1007/s13399-022-02885-4.

[29] Ji, H., Lv, P. (2020). Mechanistic insights into the lignin dissolution behaviors of a recyclable acid hydrotrope, deep eutectic solvent (DES), and ionic liquid (IL). *Green Chemistry*, 22(4), 1378–1387. DOI: 10.1039/C9GC02760B.

[30] Oh, Y., Park, S., Jung, D., Oh, K.K., Lee, S.H. (2020). Effect of hydrogen bond donor on the choline chloride-based deep eutectic solvent-mediated extraction of lignin from pine wood. *International Journal of Biological Macromolecules*, 165, 187–197. DOI: 10.1016/j.ijbiomac.2020.09.145.

[31] Popa-Tudor, I., Faraon, V.A., Oancea, F., Constantinescu-Aruxandei, D. (2022). Applications of Deep Eutectic Solvents for Lignin Extraction. In: *The 17th International Symposium "Priorities of Chemistry for a Sustainable Development" PRIOCHEM*, p. 36. DOI: 10.3390/chemproc2022007036.

[32] Wei, Q., Shi, C., Wang, D., Yang, J., Shi, Z., Wen, J.-L., Yang, H.-Y. (2025). Metal chloride mediated choline chloride-lactic acid deep eutectic solvent pretreatment of bamboo for improved cellulose saccharification and lignin recovery. *International Journal of Biological Macromolecules*, 305, 141107. DOI: 10.1016/j.ijbiomac.2025.141107.

[33] Li, P., Qian, W., Wu, S., Liu, Y. (2025). Acidic Deep Eutectic Solvents for Lignocellulose Pretreatment: Insights into Lignin Extraction Efficiency and Structural Transformation. *ACS Sustainable Chemistry & Engineering*, 13(26), 9987–10018. DOI: 10.1021/acssuschemeng.5c02184.

[34] Ji, H., Lv, P. (2020). Mechanistic insights into the lignin dissolution behaviors of a recyclable acid hydrotrope, deep eutectic solvent (DES), and ionic liquid (IL). *Green Chemistry*, 22(4), 1378–1387. DOI: 10.1039/C9GC02760B.

[35] Zhang, Z., Xu, J., Xie, J., Zhou, Z., Zhu, S., Li, J., Zhang, W., Chen, K. (2024). Model-based process intensification of deep eutectic solvent treatment of eucalyptus slabs for lignin extraction and pulp production. *Chemical Engineering Journal*, 490. DOI: 10.1016/j.cej.2024.151745.

[36] Li, W.X., Xiao, W.Z., Yang, Y.Q., Wang, Q., Chen, X., Xiao, L.P., Sun, R.C. (2021). Insights into bamboo delignification with acidic deep eutectic solvents pretreatment for enhanced lignin fractionation and valorization. *Industrial Crops and Products*, 170. DOI: 10.1016/j.indcrop.2021.113692.

[37] Xu, X., Gai, J., Li, Y., Zhang, Z., Wu, S., Song, K., Hu, J., Chu, Q. (2024). Integrated acetic acid and deep eutectic solvent pretreatment on poplar for co-production of xylo-oligosaccharides, fermentable sugars and lignin antioxidants/adsorbents. *International Journal of Biological Macromolecules*, 259. DOI: 10.1016/j.ijbiomac.2023.129138.

[38] Varilla-Mazaba, A., Raggazo-Sánchez, J.A., Calderón-Santoyo, M., Gómez-Rodríguez, J., Aguilar-Uscanga, M.G. (2022). Optimization of lignin extraction by response surface methodology from sugarcane bagasse using deep eutectic solvents (DES). *Industrial Crops and Products*, 184, 115040. DOI: 10.1016/J.INDCROP.2022.115040.

[39] Zhang, Y., Guo, Y., Xie, X., Chernyshev, V.M., Liu, Y., Qi, W. (2023). Effects of phosphoric acid/hydrogen peroxide, ammonia/hydrogen peroxide and deep eutectic solvent pretreatments on component separation and enzymatic saccharification of Glycyrrhiza residue. *Industrial Crops and Products*, 196, 116525. DOI: 10.1016/J.INDCROP.2023.116525.

[40] Yiin, C.L., Yusup, S., Quitain, A.T., Uemura, Y., Sasaki, M., Kida, T. (2018). Delignification kinetics of empty fruit bunch (EFB): a sustainable and green pretreatment approach using malic acid-based solvents. *Clean Technologies and Environmental Policy*, 20(9), 1987–2000. DOI: 10.1007/s10098-018-1592-5.

[41] Wadchasit, P., Suksong, W., O-Thong, S., Nuithitikul, K. (2021). Development of a novel reactor for simultaneous production of biogas from oil-palm empty fruit bunches (EFB) and palm oil mill effluents (POME). *Journal of Environmental Chemical Engineering*, 9(3). DOI: 10.1016/j.jece.2021.105209.

[42] Ruiz, H.A., Galbe, M., Garrote, G., Ramirez-Gutierrez, D.M., Ximenes, E., Sun, S.-N., Lachos-Perez, D., Rodríguez-Jasso, R.M., Sun, R.-C., Yang, B., Ladisch, M.R. (2021). Severity factor kinetic model as a strategic parameter of hydrothermal processing (steam explosion and liquid hot water) for biomass fractionation under biorefinery concept. *Bioresource Technology*, 342, 125961. DOI: 10.1016/j.biortech.2021.125961.

[43] Abouelela, A.R., Nakasu, P.Y.S., Hallett, J.P. (2023). Influence of Pretreatment Severity Factor and Hammett Acidity on Softwood Fractionation by an Acidic Protic Ionic Liquid. *ACS Sustainable Chemistry and Engineering*, 11(6), 2404–2415. DOI: 10.1021/acssuschemeng.2c06076.

[44] Ma, Q., Zhu, J., Gleisner, R., Yang, R., Zhu, J.Y. (2018). Valorization of Wheat Straw Using a Recyclable Hydrotrope at Low Temperatures (≤90 °C). *ACS Sustainable Chemistry and Engineering*, 6(11), 14480–14489. DOI: 10.1021/acssuschemeng.8b03135.

[45] Wijaya, C., Sangadji, N.L., Muharja, M., Widjaja, T., Riadi, L., Elaine, E., Lau, R., Widjaja, A. (2025). Prediction by a modified severity factor in $FeCl_3$-catalyzed hydrothermal fractionation of coconut husk: Enhancing hemicellulose hydrolysis and enzymatic digestibility of cellulose. *Bioresource Technology Reports*, 102282. DOI: 10.1016/j.biteb.2025.102282.

[46] Wijaya, C., Sangadji, N.L., Muharja, M., Widjaja, T., Riadi, L., Widjaja, A. (2025). An integrated green fractionation of coconut husk: Hydrothermal and deep eutectic solvent pretreatment for enhanced sugar and lignin production. *Bioresource Technology Reports*, 29, 102078. DOI: 10.1016/j.biteb.2025.102078.

[47] Wang, R., Wang, K., Zhou, M., Xu, J., Jiang, J. (2021). Efficient fractionation of moso bamboo by synergistic hydrothermal-deep eutectic solvents pretreatment. *Bioresource Technology*, 328(January), 124873. DOI: 10.1016/j.biortech.2021.124873.

[48] Alvarez-Vasco, C., Ma, R., Quintero, M., Guo, M., Geleynse, S., Ramasamy, K.K., Wolcott, M., Zhang, X. (2016). Unique low-molecular-weight lignin with high purity extracted from wood by deep eutectic solvents (DES): A source of lignin for valorization. *Green Chemistry*, 18(19), 5133–5141. DOI: 10.1039/c6gc01007e.

[49] Zhu, W., Houtman, C.J., Zhu, J.Y., Gleisner, R., Chen, K.F. (2012). Quantitative predictions of bioconversion of aspen by dilute acid and SPORL pretreatments using a unified combined hydrolysis factor (CHF). *Process Biochemistry*, 47(5), 785–791. DOI: 10.1016/j.procbio.2012.02.012.

[50] Jiang, X., Zhai, R., Li, H., Li, C., Deng, Q., Jin, M. (2023). Understanding acid hydrolysis of corn stover during densification pretreatment for quantitative predictions of enzymatic hydrolysis efficiency using modified pretreatment severity factor. *Bioresource Technology*, 386, 129487. DOI: 10.1016/j.biortech.2023.129487.

[51] Sangadji, N.L., Wijaya, C., Sangian, H.F., Widjaja, A. (2024). Optimization of Ultrasound-enhanced Subcritical Water Hydrolysis of Oil Palm Empty Fruit Bunch for the Production of Fermentable Sugar. *Periodica Polytechnica Chemical Engineering*, 68(2), 203–215. DOI: 10.3311/PPch.23183.

[52] Lin, W., Xing, S., Jin, Y., Lu, X., Huang, C., Yong, Q. (2020). Insight into understanding the performance of deep eutectic solvent pretreatment on improving enzymatic digestibility of bamboo residues. *Bioresource Technology*, 306. DOI: 10.1016/j.biortech.2020.123163.

[53] Yan, B., Fu, Y., Ding, W., Shi, G., Wang, Z., Zhang, S. (2024). Integrated dilute acid-ternary deep eutectic solvents treatment for efficient component separation and sugar platform from lignocellulose. *Industrial Crops and Products*, 222. DOI: 10.1016/j.indcrop.2024.119808.

[54] Bai, Y., Zhang, X.F., Wang, Z., Zheng, T., Yao, J. (2022). Deep eutectic solvent with bifunctional Brønsted-Lewis acids for highly efficient lignocellulose fractionation. *Bioresource Technology*, 347. DOI: 10.1016/j.biortech.2022.126723.

[55] Guo, Y., Xu, L., Shen, F., Hu, J., Huang, M., He, J., Zhang, Y., Deng, S., Li, Q., Tian, D. (2022). Insights into lignocellulosic waste fractionation for lignin nanospheres fabrication using acidic/alkaline deep eutectic solvents. *Chemosphere*, 286, 131798. DOI: 10.1016/j.chemosphere.2021.131798.

[56] Hong, S., Shen, X.J., Pang, B., Xue, Z., Cao, X.F., Wen, J.L., Sun, Z.H., Lam, S.S., Yuan, T.Q., Sun, R.C. (2020). In-depth interpretation of the structural changes of lignin and formation of diketones during acidic deep eutectic solvent pretreatment. *Green Chemistry*, 22(6), 1851–1858. DOI: 10.1039/d0gc00006j.

[57] Miao, G., Ge, F., Hu, Y., Li, H., Yu, S., He, Y., Chen, S., Xu, F., Chen, Z., Xu, J. (2025). Mechanisms and mass-transfer kinetics of hemicellulose and lignin dissolution during deep eutectic solvent pretreatment. *AIChE Journal*. 7(2), e70116. DOI: 10.1002/aic.70116

[58] Huo, D., Sun, Y., Yang, Q., Zhang, F., Fang, G., Zhu, H., Liu, Y. (2023). Selective degradation of hemicellulose and lignin for improving enzymolysis efficiency via pretreatment using deep eutectic solvents. *Bioresource Technology*, 376. DOI: 10.1016/j.biortech.2023.128937.

[59] Zhou, M., Lv, M., Cai, S., Tian, X. (2023). Effects of enzymatic hydrolysis and physicochemical properties of lignocellulose waste through different choline based deep eutectic solvents (DESs) pretreatment. *Industrial Crops and Products*, 195, 116435. DOI: 10.1016/j.indcrop.2023.116435.

[60] Ma, C.Y., Xu, L.H., Zhang, C., Guo, K.N., Yuan, T.Q., Wen, J.L. (2021). A synergistic hydrothermal-deep eutectic solvent (DES) pretreatment for rapid fractionation and targeted valorization of hemicelluloses and cellulose from poplar wood. *Bioresource Technology*, 341(July), 125828. DOI: 10.1016/j.biortech.2021.125828.

[61] Gao, Q., Tang, Z., He, Y.C. (2025). Valorization of wheat straw through enhancement of cellulose accessibility, xylan elimination and lignin removal by choline chloride:p-toluenesulfonic acid pretreatment. *International Journal of Biological Macromolecules*, 301. DOI: 10.1016/j.ijbiomac.2025.140335.

[62] Wang, Z.K., Hong, S., Wen, J. long, Ma, C.Y., Tang, L., Jiang, H., Chen, J.J., Li, S., Shen, X.J., Yuan, T.Q. (2020). Lewis Acid-Facilitated Deep Eutectic Solvent (DES) Pretreatment for Producing High-Purity and Antioxidative Lignin. *ACS Sustainable Chemistry and Engineering*, 8(2), 1050–1057. DOI: 10.1021/acssuschemeng.9b05846.

[63] Li, H., Li, X., You, T., Li, D., Nawaz, H., Zhang, X., Xu, F. (2021). Insights into alkaline choline chloride-based deep eutectic solvents pretreatment for Populus deltoides: Lignin structural features and modification mechanism. *International Journal of Biological Macromolecules*, 193, 319–327. DOI: 10.1016/J.IJBIOMAC.2021.10.134.

[64] Shen, X.J., Wen, J.L., Mei, Q.Q., Chen, X., Sun, D., Yuan, T.Q., Sun, R.C. (2019). Facile fractionation of lignocelluloses by biomass-derived deep eutectic solvent (DES) pretreatment for cellulose enzymatic hydrolysis and lignin valorization. *Green Chemistry*, 21(2), 275–283. DOI: 10.1039/c8gc03064b.

[65] Wang, Z.K., Li, H., Lin, X.C., Tang, L., Chen, J.J., Mo, J.W., Yu, R.S., Shen, X.J. (2020). Novel recyclable deep eutectic solvent boost biomass pretreatment for enzymatic hydrolysis. *Bioresource Technology*, 307(February), 123237. DOI: 10.1016/j.biortech.2020.123237.

[66] Wang, R., Wang, K., Zhou, M., Xu, J., Jiang, J. (2021). Efficient fractionation of moso bamboo by synergistic hydrothermal-deep eutectic solvents pretreatment. *Bioresource Technology*, 328, 124873. DOI: 10.1016/J.BIORTECH.2021.124873.

[67] Jose, S., B., S.B. (2023). Optimization of ultrasonication assisted alkaline delignification of coir pith using response surface methodology. *Bioresource Technology Reports*, 21, 101330. DOI: 10.1016/j.biteb.2023.101330.

[68] Gundupalli, M.P., Tantayotai, P., Panakkal, E.J., Chuetor, S., Kirdponpattara, S., Thomas, A.S.S., Sharma, B.K., Sriariyanun, M. (2022). Hydrothermal pretreatment optimization and deep eutectic solvent pretreatment of lignocellulosic biomass: An integrated approach. *Bioresource Technology Reports*, 17, 100957. DOI: 10.1016/j.biteb.2022.100957.

[69] Sunar, S.L., Oruganti, R.K., Bhattacharyya, D., Shee, D., Panda, T.K. (2024). Deep eutectic solvent pretreatment of sugarcane bagasse for efficient lignin recovery and enhanced enzymatic hydrolysis. *Journal of Industrial and Engineering Chemistry*, 139, 539–553. DOI: 10.1016/j.jiec.2024.05.030.

[70] Hou, S., Shen, B., Zhang, D., Li, R., Xu, X., Wang, K., Lai, C., Yong, Q. (2022). Understanding of promoting enzymatic hydrolysis of combined hydrothermal and deep eutectic solvent pretreated poplars by Tween 80. *Bioresource Technology*, 362. DOI: 10.1016/j.biortech.2022.127825.

[71] Jing, Y., Li, F., Li, Y., Jiang, D., Lu, C., Zhang, Z., Zhang, Q. (2022). Biohydrogen production by deep eutectic solvent delignification-driven enzymatic hydrolysis and photo-fermentation: Effect of liquid–solid ratio. *Bioresource Technology*, 349. DOI: 10.1016/j.biortech.2022.126867.

[72] Tocco, D., Carucci, C., Monduzzi, M., Salis, A., Sanjust, E. (2021). Recent Developments in the Delignification and Exploitation of Grass Lignocellulosic Biomass. *ACS Sustainable Chemistry & Engineering*, 9(6), 2412–2432. DOI: 10.1021/acssuschemeng.0c07266.

[73] Wang, W., Zhu, B., Xu, Y., Li, B., Xu, H. (2022). Mechanism study of ternary deep eutectic solvents with protonic acid for lignin fractionation. *Bioresource Technology*, 363, 127887. DOI: 10.1016/J.BIORTECH.2022.127887.

[74] Peng, J., Xu, H., Wang, W., Kong, Y., Su, Z., Li, B. (2021). Techno-economic analysis of bioethanol preparation process via deep eutectic solvent pretreatment. *Industrial Crops and Products*, 172, 114036. DOI: 10.1016/J.INDCROP.2021.114036.

[75] Hong, S., Sun, X., Lian, H., Pojman, J.A., Mota-Morales, J.D. (2020). Zinc chloride/acetamide deep eutectic solvent-mediated fractionation of lignin produces high- and low-molecular-weight fillers for phenol-formaldehyde resins. *Journal of Applied Polymer Science*, 137(7). DOI: 10.1002/app.48385.

[76] Ouyang, D., Liu, T., Astimar, A.A., Lau, H.L.N., Teh, S.S., Nursyairah, J., Liu, D., Zhao, X. (2023). Model-based process intensification of dilute acid pre-hydrolysis of oil palm empty fruit bunch biomass for pretreatment and furfural production. *Bioresource Technology*, 372. DOI: 10.1016/j.biortech.2023.128626.

[77] Fatriasari, W., Ulwan, W., Aminingsih, T., Sari, F.P., Fitria, Suryanegara, L., Iswanto, A.H., Ghozali, M., Kholida, L.N., Hussin, M.H., Fudholi, A., Hermiati, E. (2021). Optimization of maleic acid pretreatment of oil palm empty fruit bunches (OPEFB) using response surface methodology to produce reducing sugars. *Industrial Crops and Products*, 171. DOI: 10.1016/j.indcrop.2021.113971.

[78] Wang, M., Fu, X., Chang, Y., Wei, J., Cui, H. (2025). Recent advancements in Deep Eutectic Solvent (DES) pretreatment: Applications, mechanisms, and integration with emerging technologies for biorefinery. *Industrial Crops and Products*, 229, 121028. DOI: 10.1016/j.indcrop.2025.121028.